Journal of Applied Phycology (2022) 34:2259–2270
https://doi.org/10.1007/s10811-022-02795-y

Phosphate-inducible poly-hydroxy butyrate production dynamics in CO_2 supplemented upscaled cultivation of engineered *Phaeodactylum tricornutum*

Matthias Windhagauer[1] · Raffaela M. Abbriano[1] · Dorothea A. Pittrich[2] · Martina A. Doblin[1]

Received: 8 February 2022 / Revised and accepted: 26 June 2022 / Published online: 9 July 2022

Abstract
Diatoms such as *Phaeodactylum tricornutum* are emerging as sustainable alternatives to traditional eukaryotic microbial cell factories. In order to facilitate a viable process for production of heterologous metabolites, a rational genetic design specifically tailored to metabolic requirements as well as optimised culture conditions are required. In this study we investigated the effect of constitutive and inducible expression of the heterologous poly-3-hydroxybutyrate (PHB) pathway in *P. tricornutum* using non-integrative episomes in 3 different configurations. Constitutive expression led to downregulation of at least one individual gene out of three (*phaA*, *phaB* and *phaC*) and was outperformed by inducible expression. To further asses and optimise the dynamics of PHB accumulation driven by the inducible alkaline phosphatase 1 promoter, we upscaled the production to lab-scale bioreactors and tested the effect of supplemented CO_2 on biomass and PHB accumulation. While ambient CO_2 cultivation resulted in a maximum PHB yield of 2.3% cell dry weight (CDW) on day 11, under elevated CO_2 concentrations PHB yield peaked at 1.7% CDW on day 8, coincident with PHB titres at 27.9 mg L^{-1} that were approximately threefold higher than ambient CO_2. With other more valuable bio-products in mind, these results highlight the importance of the genetic design as well as substrate availability to supply additional reduction equivalents to boost biomass accumulation and relieve potential enzymatic bottlenecks for improved product accumulation.

Keywords Microalgae · CO_2-cultivation · Genetic engineering · Algal biotechnology · Bioplastic

Introduction

Genetic engineering enables the efficient production of biomolecules in host organisms for the food, pharmaceutical, and chemical industry at low cost (Parekh 2004). Microalgae are emerging as sustainable platforms that combine the advantages of a microbial bio-factory with photosynthetic capabilities. The recent advancement in genetic tool development and scale-up technology make microalgae a feasible alternative to traditional host organisms such as yeast and *Escherichia coli* (Bozarth et al. 2009). *Phaeodactylum tricornutum* is a model diatom that is set apart from other microalgal systems by an advanced genetic toolkit, including an episomal expression (EE) system that uses a self-replicating extrachromosomal episome as a vector (Karas et al. 2015; Diner et al. 2016). In contrast to random genome integration (RICE), EE has the advantage of generating genetically and phenotypically more uniform clones without disrupting the native genetic configuration, as previously shown for the expression of the fluorescent protein mVenus. This allows for genetic and metabolic studies without disruption of the host's genomic structure (George et al. 2020).

Poly-hydroxy butyrate (PHB) is a biodegradable plastic compound of the class of poly-hydroxy alkanoates (PHA) and is natively produced across different microbial taxa (Price et al. 2020). Acetyl coenzyme A (AcCoA) is the natural precursor and starting point for the biosynthesis of PHB (Masood 2017). AcCoA is one of the most important metabolic intermediates in all domains of life and is involved in cellular processes like anabolic reactions, protein acetylation, enzymatic activation, energy metabolism, and biosynthesis of lipids (Pietrocola et al. 2015). *Phaeodactylum*

✉ Matthias Windhagauer
matthias.windhagauer@student.uts.edu.au

[1] Climate Change Cluster, University of Technology Sydney, 15 Broadway, Ultimo, NSW 2007, Australia

[2] The iThree Institute, University of Technology Sydney, 15 Broadway, Ultimo, NSW 2007, Australia

tricornutum is a naturally high lipid accumulator under certain stress conditions, such as nitrogen (N) and phosphate (PO_4^{3-}) limitation (Yang et al. 2013). This suggests that a large pool of AcCoA is available in this organism. Although not much is known about the mechanisms of AcCoA partitioning or its distribution within the cell, an accessible AcCoA pool suggests that after introduction of the PHB pathway into *P. tricornutum*, metabolism could be manipulated to change the fate of AcCoA for PHB production. As previously shown by Hempel et al. (2011), random genome integration of the PHB-pathway yielded 10.6% PHB per cell dry weight (CDW) in *P. tricornutum*, as opposed to approximately 25% yield in wild-type strains of cyanobacteria (Kaewbai-ngam et al. 2016; Price et al. 2020).

When heterologous pathways are expressed in a host cell, there are several factors that can be manipulated to optimise its efficiency. These can include the genetic design of the pathway itself, including regulatory sequences such as promoters and terminators, as well as growth conditions that may relieve metabolic bottlenecks. When constitutively expressing multiple genes, the use of different promoters for each gene prevents potential homologous recombination events during the assembly, and allows adjustment of gene expression levels based on the kinetics of the corresponding enzyme activities to prevent overburdening protein expression (Vogl et al. 2018). Inducible expression, on the other hand, allows for accumulation of biomass before initiating expression of the desired genes. This is a useful strategy when the product is potentially toxic to the host or expression would burden the native metabolism to a detrimental level (Paddon et al. 2013), which potentially could be the case of constitutive expression of PHB.

While the genetic design is crucial to control gene expression at desired levels, environmental growth conditions also play an important role in the optimisation of a biological system. Previous studies have focused on the influence of CO_2 concentrations on the native metabolism of *P. tricornutum* and other microalgae, most notably surrounding fatty acid (FA) biosynthesis (Yongmanitchai and Ward 1991; Chiu et al. 2009; Wu et al. 2015, 2019; Megía-Hervás et al. 2020). Elevated CO_2 levels result in higher biomass production as well as increased total FA content and higher eicosapentaenoic acid (EPA) levels (Yongmanitchai and Ward 1991). A few microalgal studies have reported a CO_2-induced increase of NADPH through the oxidative pentose phosphate pathway (OPPP), which is the main source of reducing agents for lipid synthesis in the cytosol (Xiong et al. 2010); Wu et al. 2015. The second enzyme of the PHB synthesis pathway, the acetoacetyl-CoA reductase, has a requirement for NADPH to catalyse the reduction of acetoacetyl-CoA into 3-hydroxybutanoyl-CoA (Wakil and Bressler 1962; Poirier 2003). Therefore, cultivation of genetically modified diatom cells in CO_2 supplemented conditions could potentially lead to higher PHB productivities due to increased availability of NADPH. Furthermore, unlimited availability of inorganic carbon facilitates unhindered growth and potentially higher biomass yields as opposed to when ambient CO_2 is used.

In this study, genetic and environmental factors and their impact on the expression of the codon optimised heterologous PHB (derived from the native PHB producing bacterium *Ralstonia eutropha)* were explored in the marine diatom *P. tricornutum.* First, different combinations of previously characterised constitutive promoters were evaluated, as well as the inducible alkaline phosphatase 1 (AP1) promoter. Then, the cultivation system was upscaled to gain further insight into the dynamics of PHB expression under different CO_2 concentrations. The approach and outcomes of this study may inform future genetic designs and cultivation processes for the production of high value products.

Materials and methods

DNA isolation and codon optimisation

The sequences of the genes *phaA*, *phaB* and *phaC* of the native PHB producing pathway of the β-proteobacterium *Ralstonia eutropha* were codon-optimized for the microbial eukaryote *P. tricornutum*. Codons that were abundant at 10% or less in the diatom genome were replaced by the most frequently used codon for the corresponding amino acid in *P. tricornutum*, using codon usage tables (https://www.kazusa.or.jp/codon/cgi-bin/showcodon.cgi?species=2850&aa=1&style=N, (Nakamura et al. 2000)). Furthermore, in order to enable compatibility with the uLoop cloning system, any SapI ($GCTCTTC(N)_1^v$) and BsaI ($GGTCTC(N)_1^v$) restriction sites within the coding sequence (CDS) were removed by changing the respective codons to the most frequently used alternative, as mentioned above. The resulting genes were synthesised (Twist, USA; Gene Search, Australia) and provided as plasmids. Specific overhangs were added to ensure compatibility with the uLoop cloning system.

Plasmid design and construction of episomes

For constitutive expression of the PHB pathway, we pursued two designs that employed previously characterised native promoters in *P. tricornutum* (Windhagauer et al. 2021): one which repeated the SVP promoter for each gene in the PHB biosynthesis pathway (p_pha_SVP) to aim for relatively similar level of expression for each of the transgenes, and one that utilised a different constitutive promoter for each transgene (p_pha_Nub_Pbt_SVP) to avoid any potential recombination or silencing that may occur on episomes that contain repetitive sequences (Table S1A). In addition, we designed an episome (p_pha_AP1) where each gene in the

PHB pathway was controlled by the inducible alkaline phosphatase 1 (AP1) promoter (Table S1B). This promoter is one of the few inducible promoters available in *P. tricornutum*, is highly induced by phosphate limitation (Lin et al. 2017), and has been used successfully to express heterologous products in this diatom (Fabris et al. 2020). In addition, phosphate stress has been documented to increase neutral lipid accumulation (Brembu et al. 2017; Alipanah et al. 2018), providing an opportunity to understand the relationship between PHB and lipid biosynthesis under these conditions.

Plasmids carrying a Zeocin resistance cassette, sequences for episomal replication and maintenance, and transcriptional units for genes in the PHB pathway or individual mVenus fusion genes were constructed in three consecutive steps using a Type IIS assembly with the uLoop syntax as described by Pollak et al. (2019). The genes *phaA, pha*B and *phaC* were first ligated into the pL0R_lacZ backbone and fused to either a 6xHis-FLAG tag or mVenus + 6xHis-FLAG tag to enable immunoblotting or confocal fluorescence imaging, respectively. These L0 vectors were then used to assemble L1 transcriptional units in combination with various L0 promoters, terminators, fusion proteins and tags. Table S2 summarises genetic L0 parts that were used to construct a variety of L1 plasmids. uLoop reactions were carried out in a total volume of 10 µL, containing 2.5 µL receiver plasmids (7.5 fmol μL^{-1}), 2.5 µL donor plasmid (15 fmol μL^{-1}), 0.5 µL CutSmart buffer, 0.5 µL T4 buffer, 0.25 µL T4 ligase (400u μL^{-1}), 0.5 µL SapI/BsaI (10 U μL^{-1}) and milliQ water (MQ). A thermocycler (Veriti 96 Well Thermocycler, Applied Biosystems, USA) was set to the following parameters to perform the reaction: 25 cycles of 37 °C for 3 min and 16 °C for 4 min followed by 37 °C for 10 min, 50 °C for 5 min and 80 °C for 10 min.

The assembled products were transformed into chemically competent *Escherichia coli* Top 10 cells. Colony PCRs were performed on white *E. coli* clones for L0 and L1 assemblies using uLoop specific primers (Table S3A) and GoTaq Flexi polymerase (Promega, USA) to confirm correct plasmid assemblies. Plasmid DNA was purified from *E. coli* cells (GeneJET Plasmid Miniprep Kit, Thermo Scientific, Lithuania). For L0 and L1 constructs, the correct sequence was confirmed by Sanger sequencing (Macrogen, Korea). The final L2 expression vectors were confirmed by restriction digests followed by gel electrophoresis. All L2 plasmids were assembled using the uLoop system, except for the inducible constructs controlled by the AP1 promoter, which was assembled from L1 parts using Gibson assembly.

Gibson assembly

In order to assemble the construct carrying the pathway under control of the AP1 promoter and FcpB terminator, we used the NEBuilder HiFi DNA Assembly Cloning Kit (New England Biolabs, USA) to perform a 4-fragment assembly (fragment list in Table S1B) with the pPTPBR11 backbone (Diner et al. 2016). The corresponding primers can be found in Table S3B. Transformation and plasmid DNA preparation were done as mentioned above. The resulting episome was confirmed via restriction digest and whole plasmid sequencing (MiSeq, Illumina, USA). Figure S1 shows representative plasmid maps.

Transformation

Diatom cells were transformed using bacterial conjugation as previously described (Diner et al. 2016). In short, the *E. coli* strain that contained the pTA-Mob mobilisation helper plasmid was transformed with the cargo plasmid. 10 mL of exponentially growing *E. coli* cultures ($OD_{600} = 1.2 \pm 0.4$) were concentrated via centrifugation (15,000 ×*g*, 1 min) in 80 µL SOC outgrowth medium (New England Biolabs, USA). 50 µL adjusted *E. coli* suspension were mixed with diatom cells that were plated on half strength artificial sea water (ASW; Darley and Volcani 1969) 5% LB agar plates the previous day at a concentration of 4×10^8 cells mL^{-1}. The diatom and bacteria mixture was then incubated at 30 °C in the dark for 90 min. Subsequently, the plates were transferred to room temperature and 15 µmol photons m^{-2} s^{-1} for 48 h. The cells were then scraped off the plates, suspended in 500 mL of ASW, and transferred to selection agar plates containing 100 µg mL^{-1} Zeocin. After 15 days, single colonies were transferred to 96 micro well plates containing 200 µL ASW medium and 100 µg mL^{-1} Zeocin. Cultures were sub-cultured twice before screening for PHB production via HPLC.

Cell culture

The diatom *Phaeodactylum tricornutum* strain CCAP 1005/1 was obtained from the Bigelow National Center of Marine Algae and Microbiota collection (https://ncma.bigelow.org). It was maintained in 10 mL ASW at 21 °C under continuous light (50 µmol photons m^{-2} s^{-1}) without agitation. Transformed cells were cultivated under continuous light in 50 mL of ASW and Zeocin (100 µg mL^{-1}). Fully controlled incubators (Kühner, Switzerland) were set to 21 °C with a light intensity of 200 µmol photons m^{-2} s^{-1}. Agitation of the cultures at 110 rpm kept cells suspended. For the initial screening, cells containing constitutively controlled pathways were cultivated in batch culture for 13 days. Cell lines harbouring inducibly controlled *pha* genes were washed twice on day 7 and resuspended in PO_4^{3-} deplete ASW medium in order to induce gene expression, and incubated for a further 7 days.

Bioreactor cultures were inoculated at cell densities of approx. 4×10^5 cells mL^{-1} in nutrient enriched (2x) ASW

(2 × NO_3^-, 2 × PO_4^{3-}, 2 × trace elements and 2 × vitamins) in 2.7 L (1 L working volume) DASGIP bioreactors (Eppendorf, Germany) with the following modifications for phototrophic growth: 2 light rods were fitted vertically into the reactors. External LED Hydralights (Aquaillumination, USA) were used for additional light (Figure S2). To induce expression, cultures were resuspended in P-deplete ASW (2 × NO_3^-, 2 × trace elements and 2 × vitamins) on day 5 during exponential growth. For ambient CO_2 cultivation, air was used as a CO_2 source. For enriched CO_2 cultivation, CO_2 was supplemented to air at a rate to keep the culture pH in around 8 (Table S4). In order to facilitate optimum growth without photo inhibitory effects, the light was ramped up throughout the cultivation. Daily subsamples of cells were manually counted using a Neubauer hemocytometer. Subsamples for PHB analysis were taken daily after induction.

Microscopy

In order to confirm cytosolic expression of the PHB pathway, genes were fused to mVenus and expressed individually. Diatom cells were imaged on a Delta Vision Elite Phase microscope (software: 'softWoRx') using a 100 × objective with immersion oil (refractive index 1.516). Phase contrast and fluorescent images were taken with the appropriate channels to detect chlorophyll *a* autofluorescence (Cy5 channel: excitation: 618–646 nm, emission: 654–700 nm) and mVenus fluorescence (YFP channel: excitation: 497–527 nm, emission: 537–549 nm). Composite images were generated and brightness and contrast were adjusted using the FIJI software (Schindelin et al. 2012).

Chemical analysis of PHB using HPLC

50 mL of flask culture and 6 mL subsamples of bioreactor cultures were harvested by centrifugation (3500 × *g*, 5 min), consecutively washed with 5 mL 1X phosphate buffered saline (PBS) and 5 mL ultra-pure water and subsequently lyophilised overnight at 0.1 mPa and -80 °C. After determining the cell dry weight using a digital balance (Sartorius, France) the biomass was hydrolysed in sulfuric acid (98%) at 90 °C for 2 h, which converted PHB to crotonic acid (Karr et al. 1983). The digestate was then centrifuged (≥ 15,000 × *g*, 2 min), filtered and loaded on the HPLC detection system in glass vials (column: Aminex HPX-87H, UHPLC Agilent Technologies 1290 Infinity II LC system). The UV absorbance spectrum and elution time of crotonic acid standard (Sigma Aldrich) and PHB standard (Sigma Aldrich) validated effective digestion and presence of PHB in samples.

RNA isolation and reverse transcription

To confirm transcription of PHB genes, cell lines harbouring the PHB pathway under the control of constitutively expressing promoters were analysed for *phaA*, *phaB* and *phaC* transcript abundance. 20 mL of exponentially growing diatom cells were harvested via centrifugation (4000 × *g*, 5 min), washed once with 4 mL 1X PBS, snap frozen in liquid nitrogen, and stored at -80 °C. Trizol reagent was used to extract total RNA from approximately 10^8 cells, which subsequently was purified using the RNAeasy mini purification kit (Qiagen, Germany). Genomic DNA was removed with the PureLink DNase Set (Thermo Fisher) and RNA was quantified by spectrophotometry (NanoDrop 2000, Thermo Fisher Scientific, USA). Conversion of 700 ng mRNA into cDNA was done using iScript gDNA clear cDNA Synthesis Kit (Biorad, USA) for each sample. Dilutions and RT-qPCR reactions were prepared in 348 well plates (Biorad, USA) using an Eppendorf epMotion 5075 (Eppendorf, Germany). RT-qPCR reactions had a total volume of 10 µL, including 4 µL of cDNA and 6 µL of iTaq Universal SYBR Green Supermmix (Biorad, USA) with gene specific primers (400 nM). Reactions were performed in triplicate using a CFX384 Touch Real-Time PCR Detection System (Biorad, USA) using the following protocol: initial incubation at 95 C° for 10 min, 45 cycles of 95 C°, 60 C° and 68 C° for 30 s. A melting curve was recorded after the amplification cycles for the verification of specificity to the target amplicon. Primer efficiencies were determined from a calibration curve with a primer dilution series of 3, 9, 27, 81 and 243 dilutions following a linear regression model (Pfaffl 2001). All RT-qPCR efficiencies ranged between 100 and 110%, which is regarded as valid (Fernandez et al. 2011; Ponton et al. 2011; Schliep et al. 2015; Goyen et al. 2017). To control for absence of DNA contamination in cDNA samples a no template control as well as a no reverse transcription control were included. The ribosomal protein S1 (RPS1), Histone 4 protein (H4) and hypoxanthine–guanine phosphoribosyltransferase (HPRT) were used as reference genes (Sachse et al. 2013). Relative quantities were calculated using the slope and intercept of the calculated standard curve and Cq values of samples (see equation below). Relative quantities were normalised against the geometric mean of the reference transcripts.

$$Relative\ quantity = 10^{(Cq-int)/slope}$$

Protein extraction and analysis

40 mL of exponentially growing diatom cells (3.3×10^6 – 11.6×10^6 cells mL^{-1}) were harvested by centrifugation

(4000 ×*g*, 5 min). The cell pellet was washed twice with 4 mL 1X PBS and re-pelleted at 4000 ×*g* at 4 °C for 10 min. Cells were snap frozen in liquid nitrogen and stored at -80 °C until further analysis. For protein extraction, cells were resuspended in 1 mL of lysis buffer (150 mM NaCl, 1 mM EDTA, 50 mM Tris–HCl pH 7.5, 0.1% (v/v) Triton X-100, protease inhibitor cocktail powder (Sigma Aldrich)). After sonication (Q500, QSonica, USA) for 3 min on ice, the resulting crude protein extract was centrifuged at 14,000 ×*g* and 4 °C for 30 min. The supernatant was separated and centrifuged at 20,000 ×*g* at 4 °C for 2 h. The liberated chlorophyll *a* was removed by precipitation of the protein samples in 100% acetone and redissolving it in 2.5 M urea. The Pierce BCA Protein Assay Kit was used to determine protein concentration. To separate the protein via sodium dodecyl sulfate polyacrylamide gel electrophoresis (SDS-PAGE), a total of 50 µg of protein was diluted 1:4 in Laemmli Sample buffer (Biorad, USA) supplemented with 10% v/v β-mercaptoethanol and incubated at 95 °C for 10 min. After protein separation via SDS-PAGE in Tris/glycin/SDS buffer, a Trans-Blot Turbo Transfer System (Bio-rad, USA) was used to transfer the gel (4–15% Mini-PROTEAN TGX Stain-Free Protein, Biorad) to a polyvinylidene fluoride membrane (Trans-Blot Turbo Midi PVDF Transfer Packs, BioRad). Subsequently the blotted membrane was incubated with primary (mouse anti-His antibody (1:1000 in 5% w/v skim milk in PBS + 0.1% Tween 20) and secondary antibody (rabbit anti mouse IgG antibody conjugated to horseradish peroxidase (1:5000 in 5% w/v skim milk in PBS + 0.1% Tween 20)). Clarity ECL Western Blotting Substrates (BioRad) and a ChemiDoc MP (Biorad, USA) imaging system were used to visualise the blot and thereby confirm presence of transgenic enzymes.

Screening of BODIPY stained transformed algae cells using flow cytometry

Daily subsamples of bioreactor cultures were washed in PBS, snap-frozen in liquid N_2 and stored at -80 °C until analysis. The fluorescent dye 4,4-difluoro-1,3,5,7,8-pentamethyl-4-bora-3a,4a-diaza-s-indacene (BODIPY) was used to stain non-polar lipids. Frozen samples were resuspended in ASW and incubated with 0.1 µg mL^{-1} BODIPY (BODIPY stock: 10 µg mL^{-1} in DMSO) for 5 min in the dark in 96 well round bottom plates prior to flow cytometric detection of BODIPY fluorescence. BODIPY and chlorophyll *a* were measured using 488 nm excitation laser and 690/50 and 525/40 nm fluorescence emission detectors, respectively. Chlorophyll-negative events were excluded from the analysis to account for cell debris.

Results

PHB enzymes are localised in the cytosol

Prior to expression of the entire PHB pathway in *P. tricornutum* we individually expressed protein-mVenus fusions to determine the localisation of individual enzymes in the PHB biosynthetic pathway. The subcellular localisation of transgene expression was validated using fluorescence microscopy. All three proteins localised to the cytosol, which indicates no undirected transfer of the protein into the plastid (Fig. 1).

AP1 inducible PHB pathway outperforms constitutive PHB pathway expression

To evaluate the performance of different genetic configurations, we transformed wild type *P. tricornutum* cells with episomes containing the PHB biosynthetic pathway under the control of constitutive promoters (p_pha_SVP, pha_Nub_Pbt_SVP) and the inducible promotor (p_pha_AP1). Conjugation yielded colonies for all 3 constructs. To screen for PHB-positive clones, 12 cell lines of each construct were grown in batch culture. No significant differences between transgenic cell lines and empty vector controls in cell growth or cell size were detected (Figure S3). Inducible p_pha_AP1 cell lines were induced on day 7. No PHB was detected in constitutive cultures after 14 days of batch cultivation. However, 5 of the inducible clones showed trace amounts of PHB on day 7 after induction (Figure S4) in the range of 0.25 to 0.5% cell dry weight (CDW).

Downregulation of individual genes constrains constitutive PHB synthesis

The reason for absence of PHB in cell lines harbouring the constitutively regulated PHB pathway was further investigated. After Sanger sequencing of L1 parts we confirmed successful assembly of the episomes via restriction digest (Figure S5). Therefore, we are confident that functional expression cassettes were introduced into the diatom cells. However, it is possible that constitutive expression of the pathway imposed a strong metabolic burden on the host that was counteracted by downregulation of the pathway to relieve *P. tricornutum* cells from potential negative fitness consequences, resulting in no PHB accumulation. Several mechanisms, such as posttranscriptional and posttranslational silencing, are potential strategies to shut down the expression of a problematic heterologous pathway. To identify on which level downregulation of the pathway occurred,

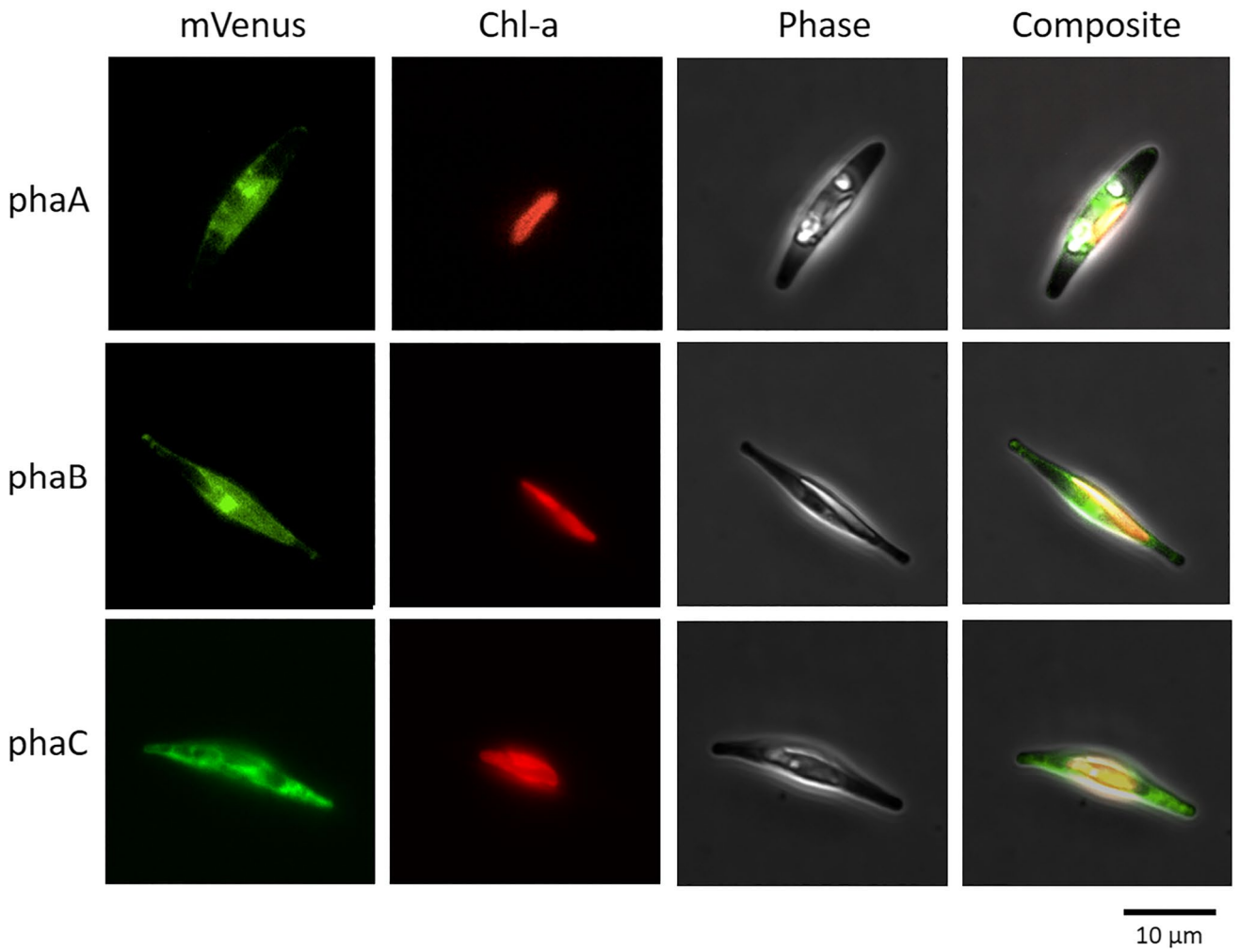

Fig. 1 Fluorescence microscopy images of cell lines expressing individual PHB-mVenus fusion genes. mVenus fluorescence and chlorophyll-*a* autofluorescence are represented in green and red, respectively

we screened the *phaA*, *phaB* and *phaC* protein and mRNA abundance in 5 randomly chosen cell lines for each of the constitutive constructs during mid exponential phase. Immunoblotting of total protein extracts showed only parts of the pathway were expressed (Fig. 2). This was in stark contrast to expression in the inducible cell line G8 which demonstrated 3 specific bands corresponding to the molecular weight of the proteins phaA, phaB and phaC (Figure S6).

As described in previous studies, transcript levels do not always correlate with protein levels (Barrett et al. 2012; Vogel and Marcotte 2012; Kendrick 2014; McManus et al. 2015; Liu et al. 2016; Windhagauer et al. 2021). None of the samples that show transcript levels close to zero result in a protein band, although some genes are transcribed but do not yield detectable amounts of protein (*phaA*: E2 and E10, *phaC:* E7) (Fig. 2, Figure S6). Furthermore, transcript levels for the lowest and highest expressed gene that translate into a detectable amount of protein (*phaB* in C10 and *phaA* in E4) vary by a factor of approximately 500. Overall, transcript levels appear to be highest for *phaA* and lowest for *phaB,* but protein bands for phaB appear to be the most intense Figure S6.

PHB synthesis correlates with cell growth

To understand the dynamics of recombinant PHB accumulation in *P. tricornutum* and gain insight into host cell metabolism, we upscaled the cultivation of the inducible p_pha_AP1 cell lines to 1 L benchtop reactors to allow daily subsampling (Fig. 3). Cultures were subjected to 2 different conditions: supplemented CO_2 and ambient atmospheric CO_2. PHB synthesis was induced on day 5 by resuspending the cultures in P-deplete medium. In CO_2 supplemented conditions, a maximum cell density of approximately 1.8×10^8 cells mL^{-1} was reached on day 9, while biomass continued to increase until day 12 (Fig. 3a). Ambient CO_2 cultures

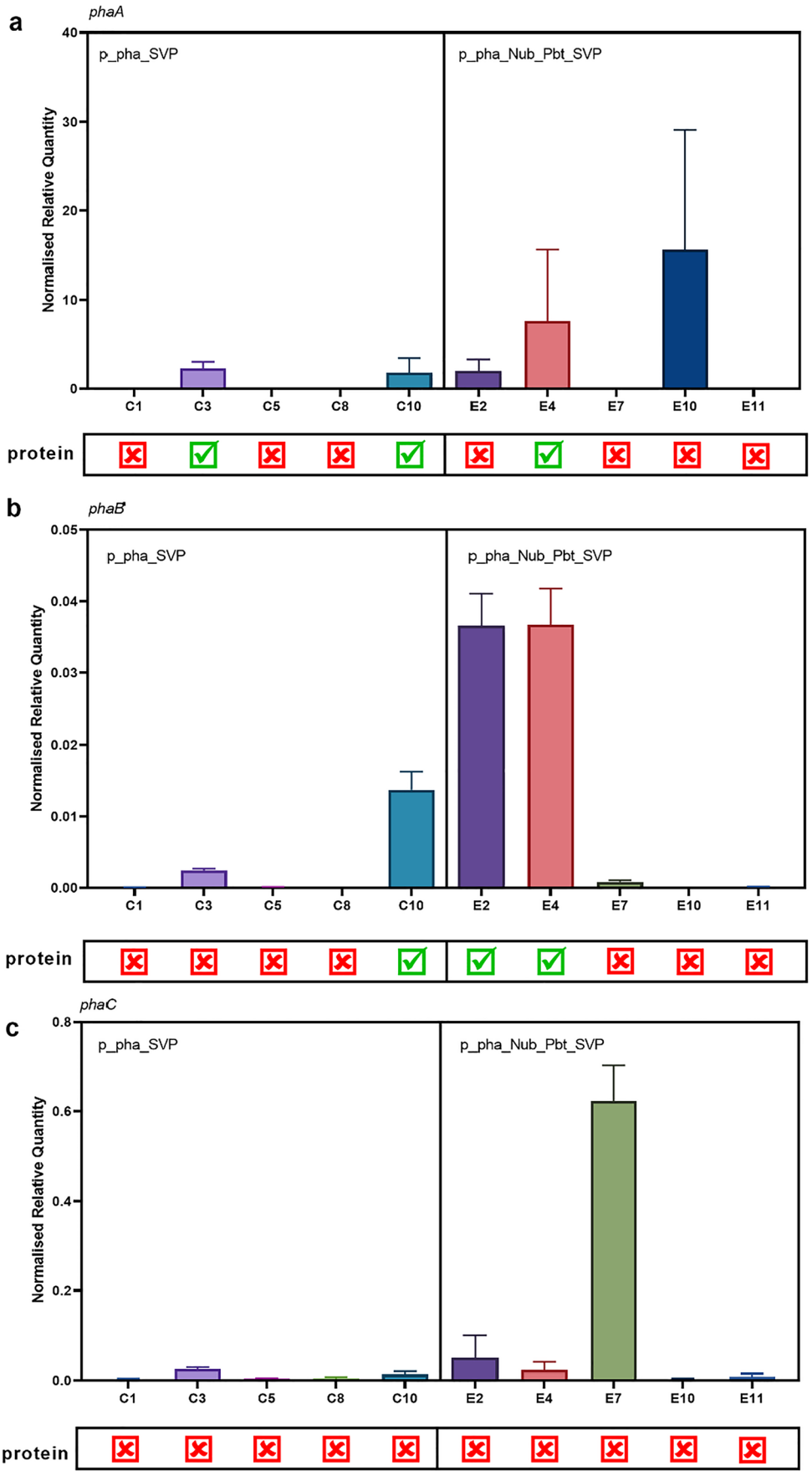

Fig. 2 RT-qPCR results and Western Blot results of selected constitutive cell lines. Normalised relative quantities of gene transcripts are represented as bar plots. Presence of the corresponding enzymes in detectable quantities is indicated below each bar plot by green ticks. a: Normalised relative quantity of *phaA*. b: Normalised relative quantity of *phaB*. c: Normalised relative quantity of *phaC*. Labels on the x-axis represent individual cell lines. The corresponding Western blot images can be found in Figure S6. Error bars represent standard deviations of technical replicates

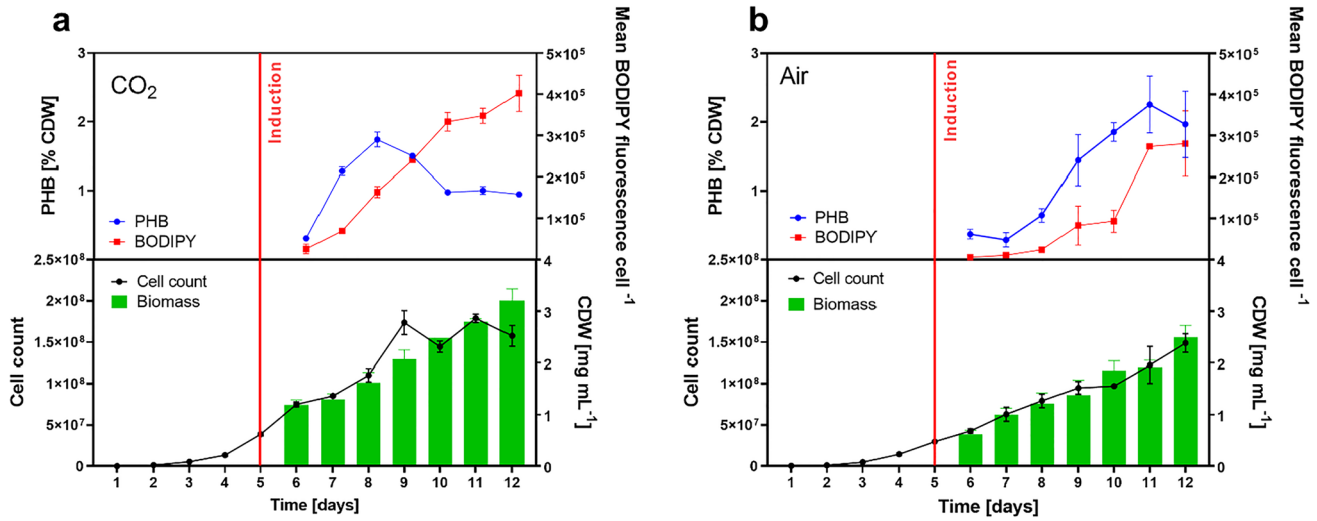

Fig. 3 Dynamics of PHB accumulation and growth of G8 cultivated under CO_2 and air in bioreactors. **Panel a** shows duplicate data of bioreactors supplemented with CO_2. **Panel b** shows duplicate data of bioreactors run with air as a gas supply. Error bars represent ranges ($n = 2$)

reached a maximum cell density of approximately 1.5×10^8 cells mL^{-1} by day 12 coincident with a continuous increase in biomass (Fig. 3b). The CDW follows a similar trend in both conditions. Final biomass yields were 3.2 ± 0.3 and 2.5 ± 0.3 mg mL^{-1} for supplemented and ambient CO_2, respectively. The continued growth after resuspension in P-deplete medium was expected, as *P. tricornutum* has been shown to mobilise and recycle intracellular P-stores and scavenge extracellular organic P-compounds, allowing sustained cell division (Huang et al. 2019; Dell'Aquila and Maier 2020).

The CO_2 supplemented PHB yield peaked at $1.7 \pm 0.2\%$ CDW 3 days after induction (day 8) followed by a decrease to $0.95 \pm 0.04\%$ by day 12. Under ambient CO_2, PHB accumulated gradually, reaching a maximum of $2.3 \pm 0.6\%$ CDW on day 11. Subsequently, the PHB yield dropped to a final of $2.0 \pm 0.7\%$ on day 12. CO_2 supplementation accelerated PHB production but did not elevate it beyond ambient CO_2 yields. The average BODIPY fluorescence per cell in the CO_2 cultures increased almost linearly throughout the induction phase to $4.0 \times 10^5 \pm 0.6 \times 10^5$ relative fluorescent units (RFU), while in ambient cultures BODIPY fluorescence only slowly increased over the first 5 days of induction followed by a steep increase on day 6, reaching its maximum of $2.8 \times 10^5 \pm 1.1 \times 10^5$ RFU. Although PHB gets co-stained with lipids and BODIPY fluorescence can't be deconvoluted into the two contributing components, it is likely the signal is dominated by lipids, as they comprise up to ~ 50% CDW compared to ~ 1% for PHB (Butler et al. 2020).

PHB accumulation and cell growth appear to be correlated in both CO_2 conditions. Following induction, PHB started to accumulate while the cells were still dividing. Supplemented with CO_2, CDW continued to increase even after cell division ceased on day 9 (Fig. 3a), indicating an increase in individual cell mass. The gradual increase of CDW was accompanied by a concomitant increase in BODIPY fluorescence, which is consistent with neutral lipid accumulation due to P-limitation (Feng et al. 2015; Brembu et al. 2017; Alipanah et al. 2018; Huang et al. 2019). After day 9, we also observed a decrease in PHB yield. As *P. tricornutum* does not possess the enzymes to degrade PHB, the drop in PHB yield is related to the observed increase in CDW and neutral lipids (i.e. as cells increased in weight, PHB per cell diminished). Under ambient CO_2 concentrations, the culture became C-limited (inferred from the pH increase (Figure S7)) and accumulated neutral lipids at a slower rate (Fig. 3b) until available P was potentially recycled, allowing PHB to accumulate without the direct competition of lipid biosynthesis over 6 days. In addition, final BODIPY fluorescence under ambient CO_2 was more than 10 times lower compared to enriched CO_2, indicating less lipid accumulation in the same time period.

Supplemented CO_2 increases volumetric PHB productivity early after induction

When comparing the efficiency of heterologous PHB production in bioreactors at different carbon supply rates, CO_2 supplementation was the more productive system over the first 3 days (Fig. 4). By day three post-induction, 27.9 ± 2.5 mg L^{-1} PHB had accumulated under supplemented CO_2 compared to only 8.0 ± 3.6 mg L^{-1} P under ambient CO_2. After day 3 PHB concentration remained stable between approximately 24 and 30 mg L^{-1} for supplemented CO2, while under ambient CO_2 concentrations PHB titres reached a maximum of approximately 48 mg L^{-1}.

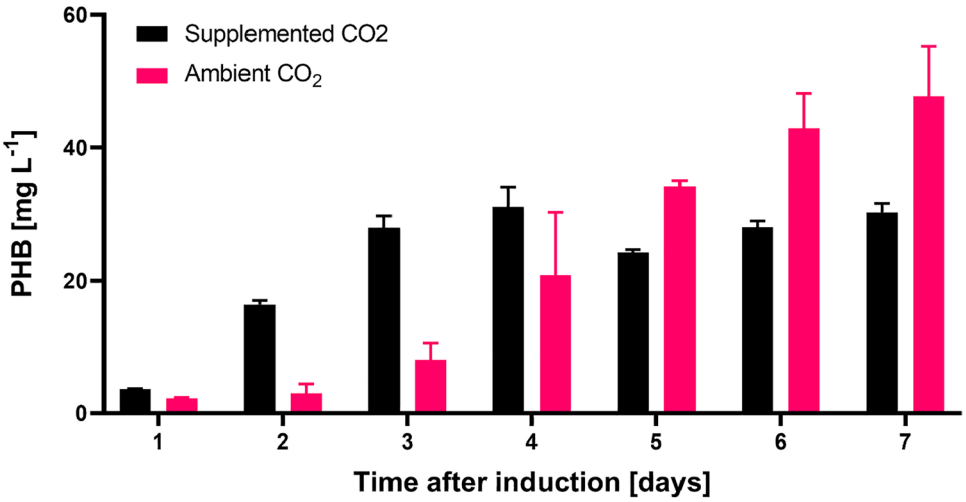

Fig. 4 PHB titres of cell line G8 in CO_2 supplemented and ambient air cultures following induction by P-limitation. Error bars indicate the ranges ($n = 2$)

The additional carbon in the system allowed for faster cell growth, resulting in rapid PHB synthesis and higher cell densities in less time.

Discussion

This study explored the effect of various promoter configurations on the expression of a heterologous pathway in the diatom *P. tricornutum*. Our data suggest that the level and timing of pathway expression is key to obtaining the desired metabolic outcome.

The observation that constitutive promotors failed to produce PHB suggests that *P. tricornutum* employs a variety of strategies, including post-transcriptional and transcriptional mechanisms, to regulate the expression of foreign DNA. For example, transcripts that do not translate into protein (as observed in all of our constitutive cell lines) might be explained by posttranscriptional silencing (Fig. 2). Small non-coding RNAs including microRNA have been reported to be involved in the regulation of cellular activities including post-transcriptional gene silencing via RNAi (Carthew 2006; De Riso et al. 2009; Huang et al. 2011; Doron et al. 2016) and could potentially target native untranslated regions (UTR) on our expressed transcripts. Previous research has also investigated transcriptional gene silencing mechanisms in *P. tricornutum*. De Riso et al. (2009) found that transcription of transgenic DNA can be inhibited by methylation of transgenes integrated into genomic DNA. Methylation of the *pha* genes and/or the corresponding up- and downstream UTRs may explain samples with low transcript abundance. Further research is necessary to understand potential transcriptional and post-transcriptional regulation mechanisms of transgenes introduced to *P. tricornutum* on plasmids.

The focus of this study was to examine EE as a proof of principle and explore the dynamics and regulatory control of PHB synthesis, not to maximise yields to industrially relevant levels. The PHB yields we obtained in the inducible cell lines were low compared to 10.6% CDW that was reported for *P. tricornutum* by Hempel et al. (2011). Nevertheless, the divergence in our results may be explained by several factors. First, Hempel et al. used the Nitrate Reductase (NR) promoter to control gene expression, whereas we used the AP1 promoter. Different promoters drive expression at different levels and may have been responsible for different PHB yields. Second, different environmental conditions are required to induce the NR and AP1 promoters. While the NR promoter is induced by changing the N-source from Ammonium (NH_4^+) to Nitrate (NO_3^-), P-depletion leads to activation of the AP1 promoter. However, P-limitation also induces native lipid synthesis and accumulation in *P. tricornutum*, which potentially competes for the same AcCoA precursors as used in the heterologous PHB pathway (Brembu et al. 2017; Alipanah et al. 2018). Under nutrient deplete conditions, the host cell may preferentially reroute AcCoA away from PHB towards FA synthesis and thus limit PHB yield. Third, Hempel et al. (2011) randomly integrated the pathway into the host genome, while EE was employed in this study. A previous comparison of RICE and EE showed that while RICE resulted in higher gene expression potentially due to position effects and higher gene copy number, EE resulted in genetically more consistent transgenic cell lines without disrupting the host genome (George et al. 2020). Even though EE potentially results in lower heterologous expression, its metabolic effects on the host are more consistent, resulting in more consistent phenotypes, less inter-clonal heterogeneity and therefore lower screening efforts.

Furthermore, several studies on the kinetics of the PHB pathway have suggested that the second reaction in the pathway (*phaB*) is the rate limiting step due to its dependence on reducing equivalents (Lee et al. 1996; Chohan and Copeland 1998; Centeno-Leija et al. 2014; Sacomboio et al.

2017; Alsiyabi et al. 2021). In *P. tricornutum*, increased CO_2 availability leads to an upregulation of the oxidative pentose phosphate pathway (OPPP) and therefore to an increased pool of cytosolic NADPH (Wu et al. 2015). This could potentially relieve the bottleneck of PHB synthesis through more rapid conversion of acetoacetyl-CoA into 3-hydroxybutanoyl-CoA, potentially explaining faster accumulation of PHB in supplemented as opposed to ambient CO_2 conditions.

The bioreactor experiments provided added insight into the dynamics of PHB production because they allowed daily sampling. The data suggest a potential competitive relationship between lipid and PHB biosynthesis over the precursor AcCoA, which may preferably be shunted towards FA synthesis and elongation, rather than being converted to PHB. Understanding the regulatory mechanisms of transgenic metabolic pathways that compete with native pathways would be an insightful area of further research.

Conclusions

In order to generate reliable yields from cell factories, a rational genetic design is crucial to avoid running into competition with native metabolism. The choice of constitutive versus inducible promoters is an important factor when the pathway potentially poses a big metabolic burden for the host. In addition, the type of induction condition for gene expression has implications for the productivity and dynamics of the system. This study shows that there is need for an expanded set of inducible promoters in *P. tricornutum*, such as the *lac* operon in E. coli or the *CUP1* promoter in yeast, or the just recently published DIG-inducible and XVE/OlexA systems. All of these promotors rely on the addition of certain compounds to cultivated cells and can be induced by conditions that do not impose significant changes to the host's metabolic network/central carbon metabolism, and thereby prioritise the expression of a desired pathway. While we attempted to engineer a system that did not rely on inducible production, we found that none of the 24 constitutive promotor cell lines tested yielded our target product.

When expressing products of pathways that act as carbon or electron sinks, the application of increased CO_2-concentrations is sensible for increased inorganic carbon availability as well as for the supply of reductive equivalents. Therefore, optimised culturing conditions paired with an appropriate genetic design are the prerequisites before successful upscaling of bio-production processes using micro algae as sustainable cell factories. Keeping in mind that high value products such as terpenoids and therapeutic recombinant proteins can be expressed in *P. tricornutum*, the strategies implemented in this study can be employed and further optimised to establish diatoms as viable industrial expression systems.

Supplementary Information The online version contains supplementary material available at https://doi.org/10.1007/s10811-022-02795-y.

Acknowledgements We thank Dr. Michele Fabris, Dr. Dominik Kopp and Dr. Artur Wlodarczyk for their scientific input; Dr. Chris Dupont and Dr. Bernardo Pollak (J. Craig Venter Institute) for kindly supplying genetic parts of the uLoop cloning systems; Dr. Unnikrishnan Kuzhiumparambil and Taya Lapshina for their technical assistance with chemical analysis. We acknowledge the use of the Delta Vision Elite Phase microscope in the Microbial Imaging Facility at the i3 institute in the Faculty of Science at the University of Technology Sydney.

Authors contributions Matthias Windhagauer, Raffaela M. Abbriano and Martina A. Doblin contributed to the study conception and design. Material preparation, data collection and analysis were performed by Matthias Windhagauer. Fluorescence microscopy was performed by Dorothea A. Pittrich. The first draft of the manuscript was written by Matthias Windhagauer. Raffaela M. Abbriano and Martina A. Doblin edited previous versions of the manuscript. All authors read and approved the final manuscript.

Funding Open Access funding enabled and organized by CAUL and its Member Institutions This study was facilitated by an International Research Scholarship by the University of Technology Sydney awarded to MW as well as research funding by the Faculty of Science and UTS:C3.

Data availability statement The datasets generated during and analysed during the current study are available from the corresponding author on reasonable request.

Declarations

Statement of competing interest The authors have no competing or financial interests to declare that are relevant to the content of this article.

References

Alipanah L, Winge P, Rohloff J, Najafi J, Brembu T, Bones AM (2018) Molecular adaptations to phosphorus deprivation and comparison with nitrogen deprivation responses in the diatom *Phaeodactylum tricornutum*. PLoS One 13:e0193335

Alsiyabi A, Brown B, Immethun C, Long D, Wilkins M, Saha R (2021) Synergistic experimental and computational approach identifies novel strategies for polyhydroxybutyrate overproduction. Metab Eng 68:1–13

Barrett LW, Fletcher S, Wilton SD (2012) Regulation of eukaryotic gene expression by the untranslated gene regions and other non-coding elements. Cell Mol Life Sci 69:3613–3634

Bozarth A, Maier U-G, Zauner S (2009) Diatoms in biotechnology: modern tools and applications. Appl Microbiol Biotechnol 82:195–201

Brembu T, Mühlroth A, Alipanah L, Bones AM (2017) The effects of phosphorus limitation on carbon metabolism in diatoms. Philos Trans R Soc B Biol Sci 372:20160406

Butler T, Kapoore RV, Vaidyanathan S (2020) *Phaeodactylum tricornutum*: a diatom cell factory. Trends Biotechnology 38:606–622

Carthew RW (2006) Gene regulation by microRNAs. Curr Opin Genet Dev 16:203–208

Centeno-Leija S, Huerta-Beristain G, Giles-Gómez M, Bolivar F, Gosset G, Martinez A (2014) Improving poly-3-hydroxybutyrate production in *Escherichia coli* by combining the increase in the NADPH pool and acetyl-CoA availability. Antonie Van Leeuwenhoek 105:687–696

Chiu S-Y, Kao C-Y, Tsai M-T, Ong S-C, Chen C-H, Lin C-S (2009) Lipid accumulation and CO_2 utilization of *Nannochloropsis oculata* in response to CO_2 aeration. Bioresour Technol 100:833–838

Chohan SN, Copeland L (1998) Acetoacetyl Coenzyme A reductase and polyhydroxybutyrate synthesis in *Rhizobium*(Cicer) sp. strain CC 1192. Appl Environ Microbiol 64:2859–2863

Darley WM, Volcani BE (1969) Role of silicon in diatom metabolism. A silicon requirement for deoxyribonucleic acid synthesis in the diatom *Cylindrotheca fusiformis* Reimann and Lewin. Exp Cell Res 58:334–342

De Riso V, Raniello R, Maumus F, Rogato A, Bowler C, Falciatore A (2009) Gene silencing in the marine diatom *Phaeodactylum tricornutum*. Nucleic Acids Res 37:e96

Dell'Aquila G, Maier UG (2020) Specific acclimations to phosphorus limitation in the marine diatom *Phaeodactylum tricornutum*. Biol Chem 401:1495–1501

Diner RE, Bielinski VA, Dupont CL, Allen AE, Weyman PD (2016) Refinement of the diatom episome maintenance sequence and improvement of conjugation-based DNA delivery methods. Front Bioeng Biotechnol 4:65

Doron L, Segal N, Shapira M (2016) Transgene expression in microalgae—from tools to applications. Front Plant Sci 7:505

Fabris M, George J, Kuzhiumparambil U, Lawson CA, Jaramillo-Madrid AC, Abbriano RM, Vickers CE, Ralph P (2020) Extrachromosomal genetic engineering of the marine diatom *Phaeodactylum tricornutum* enables the heterologous production of monoterpenoids. ACS Synth Biol 9:598–612

Feng T-Y, Yang Z-K, Zheng J-W, Xie Y, Li D-W, Murugan SB, Yang W-D, Liu J-S, Li H-Y (2015) Examination of metabolic responses to phosphorus limitation via proteomic analyses in the marine diatom *Phaeodactylum tricornutum*. Sci Rep 5:10373

Fernandez P, Di Rienzo JA, Moschen S, Dosio GAA, Aguirrezábal LAN, Hopp HE, Paniego N, Heinz RA (2011) Comparison of predictive methods and biological validation for qPCR reference genes in sunflower leaf senescence transcript analysis. Plant Cell Rep 30:63–74

George J, Kahlke T, Abbriano RM, Kuzhiumparambil U, Ralph PJ, Fabris M (2020) Metabolic engineering strategies in diatoms reveal unique phenotypes and genetic configurations with implications for algal genetics and synthetic biology. Front Bioeng Biotechnol 8:513

Goyen S, Pernice M, Szabó M, Warner ME, Ralph PJ, Suggett DJ (2017) A molecular physiology basis for functional diversity of hydrogen peroxide production amongst *Symbiodinium* spp. (Dinophyceae). Mar Biol 164:46

Hempel F, Bozarth AS, Lindenkamp N, Klingl A, Zauner S, Linne U, Steinbüchel A, Maier UG (2011) Microalgae as bioreactors for bioplastic production. Microb Cell Fact 10:81

Huang A, He L, Wang G (2011) Identification and characterization of microRNAs from *Phaeodactylum tricornutum* by high-throughput sequencing and bioinformatics analysis. BMC Genomics 12:337

Huang B, Marchand J, Blanckaert V, Lukomska E, Ulmann L, Wielgosz-Collin G, Rabesaotra V, Moreau B, Bougaran G, Mimouni V, Morant-Manceau A (2019) Nitrogen and phosphorus limitations induce carbon partitioning and membrane lipid remodelling in the marine diatom *Phaeodactylum tricornutum*. Eur J Phycol 54:342–358

Kaewbai-ngam A, Incharoensakdi A, Monshupanee T (2016) Increased accumulation of polyhydroxybutyrate in divergent cyanobacteria under nutrient-deprived photoautotrophy: an efficient conversion of solar energy and carbon dioxide to polyhydroxybutyrate by *Calothrix scytonemicola* TISTR 8095. Bioresour Technol 212:342–347

Karas BJ, Diner RE, Lefebvre SC, McQuaid J, Phillips APR, Noddings CM, Brunson JK, Valas RE, Deerinck TJ, Jablanovic J, Gillard JTF, Beeri K, Ellisman MH, Glass JI, Hutchison CA, Smith HO, Venter JC, Allen AE, Dupont CL, Weyman PD (2015) Designer diatom episomes delivered by bacterial conjugation. Nat Commun 6:6925

Karr DB, Waters JK, Emerich DW (1983) Analysis of poly-β-hydroxybutyrate in *Rhizobium japonicum* bacteroids by ion-exclusion high-pressure liquid chromatography and UV detection. Appl Environ Microbiol 46:1339–1344

Kendrick N (2014) A gene's mRNA level does not usually predict its protein level. https://kendricklabs.com/wp-content/uploads/2016/08/WP1_mRNAvsProtein_KendrickLabs.pdf

Lee IY, Kim MK, Park YH, Lee SY (1996) Regulatory effects of cellular nicotinamide nucleotides and enzyme activities on poly(3-hydroxybutyrate) synthesis in recombinant *Escherichia coli*. Biotechnol Bioeng 52:707–712

Lin H-Y, Yen S-C, Kuo P-C, Chung C-Y, Yeh K-L, Huang C-H, Chang J, Lin H-J (2017) Alkaline phosphatase promoter as an efficient driving element for exogenic recombinant in the marine diatom *Phaeodactylum tricornutum*. Algal Res 23:58–65

Liu Y, Beyer A, Aebersold R (2016) On the dependency of cellular protein levels on mRNA abundance. Cell 165:535–550

Masood F (2017) Polyhydroxyalkanoates in the food packaging industry. In: Oprea AE, Grumezescu AM (eds) Nanotechnology Applications in Food. Academic Press, London, pp. 153–177

McManus J, Cheng Z, Vogel C (2015) Next-generation analysis of gene expression regulation–comparing the roles of synthesis and degradation. Mol Biosyst 11:2680–2689

Megía-Hervás I, Sánchez-Bayo A, Bautista LF, Morales V, Witt-Sousa FG, Segura-Fornieles M, Vicente G (2020) Scale-up cultivation of *Phaeodactylum tricornutum* to produce biocrude by hydrothermal liquefaction. Processes 8:1072

Nakamura Y, Gojobori T, Ikemura T (2000) Codon usage tabulated from international DNA sequence databases: status for the year 2000. Nucleic Acids Res 28:292

Paddon CJ, Westfall PJ, Pitera DJ, Benjamin K, Fisher K, McPhee D, Leavell MD, Tai A, Main A, Eng D, Polichuk DR, Teoh KH, Reed DW, Treynor T, Lenihan J, Jiang H, Fleck M, Bajad S, Dang G, Dengrove D, Diola D, Dorin G, Ellens KW, Fickes S, Galazzo J, Gaucher SP, Geistlinger T, Henry R, Hepp M, Horning T, Iqbal T, Kizer L, Lieu B, Melis D, Moss N, Regentin R, Secrest S, Tsuruta H, Vazquez R, Westblade LF, Xu L, Yu M, Zhang Y, Zhao L, Lievense J, Covello PS, Keasling JD, Reiling KK, Renninger NS, Newman JD (2013) High-level

semi-synthetic production of the potent antimalarial artemisinin. Nature 496:528–532
Parekh SR (2004) The GMO Handbook: Genetically Modified Animals, Microbes, and Plants in Biotechnology. Springer, Berlin
Pfaffl MW (2001) A new mathematical model for relative quantification in real-time RT–PCR. Nucleic Acids Res 29:e45
Pietrocola F, Galluzzi L, Bravo-San Pedro JM, Madeo F, Kroemer G (2015) Acetyl Coenzyme A: a central metabolite and second messenger. Cell Metab 21:805–821
Poirier Y (2003) Genetic modification of primary metabolism | Biopolymers. In: Thomas B (ed) Encyclopedia of Applied Plant Sciences. Elsevier, Oxford, pp. 477–484
Pollak B, Matute T, Nuñez I, Cerda A, Lopez C, Vargas V, Kan A, Bielinski V, von Dassow P, Dupont CL, Federici F (2019) Universal Loop assembly (uLoop): open, efficient, and species-agnostic DNA fabrication. bioRxiv 744854
Ponton F, Chapuis M-P, Pernice M, Sword GA, Simpson SJ (2011) Evaluation of potential reference genes for reverse transcription-qPCR studies of physiological responses in *Drosophila melanogaster*. J Insect Physiol 57:840–850
Price S, Kuzhiumparambil U, Pernice M, Ralph PJ (2020) Cyanobacterial polyhydroxybutyrate for sustainable bioplastic production: critical review and perspectives. J Environ Chem Eng 8:104007
Sachse M, Sturm S, Gruber A, Kroth PG (2013) Identification and evaluation of endogenous reference genes for steady state transcript quantification by qPCR in the diatom *Phaeodactylum tricornutum* with constitutive expression independent from time and light. J Endocytobiosis Cell Res 24:1–7
Sacomboio ENM, Kim EYS, Ruchaud Correa HL, Bonato P, de Oliveira Pedrosa F, de Souza EM, Chubatsu LS, Müller-Santos M (2017) The transcriptional regulator NtrC controls glucose-6-phosphate dehydrogenase expression and polyhydroxybutyrate synthesis through NADPH availability in *Herbaspirillum seropedicae*. Sci Rep 7:13546
Schindelin J, Arganda-Carreras I, Frise E, Kaynig V, Longair M, Pietzsch T, Preibisch S, Rueden C, Saalfeld S, Schmid B, Tinevez J-Y, White DJ, Hartenstein V, Eliceiri K, Tomancak P, Cardona A (2012) Fiji: an open-source platform for biological-image analysis. Nat Methods 9:676–682
Schliep M, Pernice M, Sinutok S, Bryant CV, York PH, Rasheed MA, Ralph PJ (2015) Evaluation of reference genes for RT-qPCR studies in the seagrass *Zostera muelleri* exposed to light limitation. Sci Rep 5:17051
Vogel C, Marcotte EM (2012) Insights into the regulation of protein abundance from proteomic and transcriptomic analyses. Nat Rev Genet 13:227–232
Vogl T, Kickenweiz T, Pitzer J, Sturmberger L, Weninger A, Biggs BW, Köhler E-M, Baumschlager A, Fischer JE, Hyden P, Wagner M, Baumann M, Borth N, Geier M, Ajikumar PK, Glieder A (2018) Engineered bidirectional promoters enable rapid multi-gene co-expression optimization. Nat Commun 9:3589
Wakil SJ, Bressler R (1962) Studies on the mechanism of fatty acid synthesis: X. Reduced triphosphopyridine nucleotide-acetoacetyl coenzyme A reductase. J Biol Chem 237:687–693
Windhagauer M, Abbriano RM, Ashworth J, Barolo L, Jaramillo-Madrid AC, Pernice M, Doblin MA (2021) Characterisation of novel regulatory sequences compatible with modular assembly in the diatom *Phaeodactylum tricornutum*. Algal Res 53:102159
Wu S, Gu W, Huang A, Li Y, Kumar M, Lim PE, Huan L, Gao S, Wang G (2019) Elevated CO_2 improves both lipid accumulation and growth rate in the glucose-6-phosphate dehydrogenase engineered *Phaeodactylum tricornutum*. Microb Cell Fact 18:161
Wu S, Huang A, Zhang B, Huan L, Zhao P, Lin A, Wang G (2015) Enzyme activity highlights the importance of the oxidative pentose phosphate pathway in lipid accumulation and growth of *Phaeodactylum tricornutum* under CO_2 concentration. Biotechnol Biofuels 8:78
Xiong W, Liu L, Wu C, Yang C, Wu Q (2010) ^{13}C-Tracer and gas chromatography-mass spectrometry analyses reveal metabolic flux distribution in the oleaginous microalga *Chlorella protothecoides*. Plant Physiol 154:1001–1011
Yang Z-K, Niu Y-F, Ma Y-H, Xue J, Zhang M-H, Yang W-D, Liu J-S, Lu S-H, Guan Y, Li H-Y (2013) Molecular and cellular mechanisms of neutral lipid accumulation in diatom following nitrogen deprivation. Biotechnol Biofuels 6:67
Yongmanitchai W, Ward OP (1991) Growth of and omega-3 fatty acid production by *Phaeodactylum tricornutum* under different culture conditions. Appl Environ Microbiol 57:419–425